A comparative study of the oxidation of toluene and the three isomers of xylene

Ismahane Meziane, Nicolas Delort, Olivier Herbinet, Roda Bounaceur, Frédérique Battin-Leclerc

A COMPARATIVE STUDY OF THE OXIDATION OF TOLUENE AND THE THREE ISOMERS OF XYLENE

Ismahane Meziane*, Nicolas Delort*, Olivier Herbinet, Roda Bounaceur,

Frédérique Battin-Leclerc†

Université de Lorraine, CNRS, LRGP, F-54000 Nancy, France

Published in Combustion and Flame (2023) 257, 2, 113046

https://doi.org/10.1016/j.combustflame.2023.113046

Abstract

This paper presents an experimental and modelling study of the oxidation of toluene, ortho-xylene, meta-xylene, and para-xylene in a jet-stirred reactor. In order to facilitate comparisons, the same experimental conditions were used for the four reactants, i.e. temperatures from 600 to 1100 K, a pressure of 1.07 bar, a residence time of 2 s, an initial fuel mole fraction of 0.005, and equivalence ratios of 0.5, 1 and 2. Compared to literature studies using the same type of reactor, due to higher residence time and initial fuel mole fraction, a higher number of oxygenated aromatic products was quantified and some reactivity was observed at lower temperatures, especially for ortho-xylene, which started to react from 700 K. For this fuel, the formation of phthalan, an aromatic compound including an oxetane ring and indicating low-temperature oxidation chemistry, was confirmed. A new detailed kinetic model combining literature mechanisms was proposed

* These authors contributed equally to this work.
† Corresponding author: frederique.battin-leclerc@univ-lorraine.fr

and allowed well predicting the reactivity of the four methylated benzenes of interest with an acceptable simulation of most of the quantified products. Flowrate and sensitivity analyses were made to highlight the similarities and to explain the difference of reactivity between the four investigated reactants.

Keywords: Jet-stirred reactor; xylenes; toluene; oxidation.

Novelty and significance statement

In the context of promoting biofuels derived from lignin, the novelty of this work consists in a first comparative study of the JSR oxidation of toluene and the three xylene isomers. Thanks to the use of a higher residence time (2 s) and a higher initial fuel mole fraction (0.005), main original results concern new evidences of low-temperature reactivity of o-xylene and the identification and modelling of oxygenated aromatic products, such as phthalan, 2,3-dihydrobenzofuran, or 1,3-benzodioxole.

Authors contributions

IM: bibliographical work, performed experiments, analyzed results and drew figures. ND: bibliographical work, developed the model, performed simulations, and drew figures. OH: designed and controlled experiments, and analyzed results. RB: Assessed the model. FBL: designed research, made kinetic analyses and wrote the manuscript. All: reviewed the manuscript.

1. Introduction

Methylated benzenes are an important fraction of gasolines and Diesel fuel [1]. The interest of these aromatic compounds for internal combustion engines is due to their high octane number, respectively 116, 113, 122 and 121 for toluene, ortho (o)-, meta (m)- and para (p)-xylene, which makes them commonly used as octane boosters [2]. They are also part of the molecules, which can be obtained from the catalytic depolymerization of lignin [3].

Due to their interest for engine combustion, the oxidation of toluene and xylene isomers has already been extensively studied as described in the review paper by Jin *et al.* [4] in the group of Fei Qi. Previous work included measurements of ignition delay times in shock tubes [5–10] and rapid compression machines [11–14], as well as product quantification in flow tubes [15–20] and in jet-stirred reactors (JSRs).

As shown in Table 1, three literature studies concern the JSR oxidation of toluene and four that of at least one xylene isomer. Table 1 also lists the quantified products for each work, which include hydrocarbons (HC) and oxygenated molecules. Except one study performed in Nancy concerning toluene at only three temperatures, all the other experimental studies were performed in Orléans over a wide temperature range using gas-chromatography for residence times (τ) equal or below 0.5 s and with initial fuel mole fractions equal or below 0.00375. While the Orléans studies for xylene isomers [21–23] were performed under the same conditions, it was not the case for toluene.

Table 1: Previous studies of the JSR oxidation of toluene and xylene isomers (HC stands for hydrocarbons).

Reactant	T (K)	P (atm)	φ	τ (s)	Initial fuel mole fraction	Quantified products	Ref.
Toluene	1000-1375	1	0.5, 1, 1.5	0.07, 0.1, 0.12	0.0015	H_2, CO, CO_2, C_1-C_4 HC, cyclopentadiene benzene, ethylbenzene, benzaldehyde, bibenzyl	[24]
	873, 893, 923	1	0.45, 0.9	2-13	0.017	CO, CO_2, C_1-C_4 HC, benzene, phenol, styrene, ethylbenzene, benzaldehyde, benzyl alcohol, bibenzyl	[25]
	950-1200	10	0.5, 1, 1.5	0.6	0.001	H_2, CO, CH_2O, CO_2, C_1-C_4 HC, cyclopentadiene, benzene, phenol, styrene, ethylbenzene, benzaldehyde	[26]
o-Xylene	900-1400	1	0.5, 1, 2	0.1	0.00375	CO, CH_2O, CO_2, C_1-C_4 HC, cyclopentadiene, benzene, toluene, styrene	[23]
	800-1200	10	0.5, 1, 2	0.5	0.001	CO, CH_2O, CO_2, C_1-C_4 HC, cyclopentadiene, benzene, phenol + benzaldehyde, toluene, cresol, styrene, o-methylbenzaldehyde, o-methylstyrene, benzofuran, o-phtalaldehyde, methylbenzylalcohol, indene, naphthalene	[27]
m-Xylene	900-1400	1	0.5, 1, 2	0.1	0.00375	CO, CH_2O, CO_2, C_1-C_4 HC, cyclopentadiene, benzene, benzaldehyde, toluene, styrene, m-methylstyrene	[22]
p-Xylene	900-1300	1	0.5, 1, 2	0.1	0.00375	CO, CH_2O, CO_2, C_1-C_4 HC, cyclopentadiene, benzene, benzaldehyde, toluene, styrene, p-methylstyrene	[21]

A comparison between the fuel mole fractions measured by Gail *et al.* [21–23] for the three xylene isomers (φ = 1, P = 1 atm) was drawn by Jin *et al.* [4] (Figure 20a) and compared with modelling using their model, which is an extension of that of Yuan *et al.* [28]. In this high range of temperatures, above 1050 K, o- and p-xylenes have a similar reactivity and m-xylene seems to be less reactive than the two other isomers; the agreement between experiments and simulations using the model of Jin *et al.* [4] is reasonable, but might certainly be improved in the lower temperature range.

In order to quantify the maximum number of products, the present study aims at investigating the JSR oxidation of toluene and the three xylene isomers with a longer residence time (2 s) and a higher initial fuel mole fraction (0.005) than in previous literature studies. In order to facilitate comparisons, the same initial conditions are kept in the four studies. These investigations were started at a temperature of 600 K with the aim of detecting a possible low temperature reactivity for xylenes, especially the formation of the aromatic cyclic ether, phthalan, which was previously quantified by Roubaud *et al.* [12,13] during their rapid compression machine experiments with o-xylene. Based on the toluene model of Yuan *et al.* [26,29] and that of Kukkadapu *et al.* for o- and m/p-xylene [14], a new detailed kinetic model is proposed for the oxidation of these four compounds.

2. Experimental methods

The used experimental apparatus includes a heated JSR maintained at a pressure slightly above 1 bar, the supply of reactants under gaseous phase, and the transfer of the gases leaving the reactor towards gas-chromatographs for analyses.

The geometry of the fused silica JSR, the need of using a preheating line to ensure the thermal homogeneity inside the vessel, and the heating of both parts through Thermocoax

electrical resistances has been already comprehensively detailed in many recent papers, e.g. [30,31].

After gas transfer by a heated line made in PFA polymer (provided by the Swagelock Company) to minimize wall adsorption and maintained at a temperature of 373 K to prevent condensation, three gas chromatographs (GCs) are used for the quantification of reaction products. The C_{5+} compounds, such as the four aromatic fuels, are analyzed using a GC equipped with a HP-5 capillary column and a Flame Ionization Detector (FID). The C_2-C_5 compounds are obtained on a GC fitted with a Q-Bond capillary column and a FID preceded by a methanizer. For oxygen and methane, a GC with a Carbosphere packed column, a Thermal Conductivity Detector (TCD) is used. A fourth GC equipped with both type of capillary columns (H-5 and Q-Bond) and coupled to a mass spectrometer (quadrupole) allows the identification of the produced molecules. Gaseous and liquid external standards when available are used for calibrations. For species, which cannot be directly calibrated with a standard, the effective carbon number method based on the properties of the FID with respect of the structure of the molecule is used to obtain calibration coefficients from reference species calibrated using standards. The uncertainties on the compound mole fractions are 5% for fuels and 10% for all the quantified products.

Toluene (purity ≥ 99.5%), o-xylene (purity ≥ 98%), m-xylene (purity ≥ 99%) and p-xylene (purity ≥ 99%) were provided by Merck. Helium (99.999% pure) and oxygen (99.999%) were provided by Messer. The chromatograms of the four unreacted reactants are provided in Supplementary Material (SM, see Figure S1) and shows that the reacting molecule is the only aromatic one present in the sample. The liquid fuel flow rate is controlled using a Coriolis flow controller, mixed with the carrier gas (helium), and

evaporated in a heat exchanger. Helium and oxygen flow rates are controlled using mass flow controllers.

For the four fuels, CO, CO_2 and the C_{2+} products are listed according on their retention time on the Plot-Q (Table S1 in SM) and HP-5 (Table S2) columns, mentioning if they were just detected, or if their actual quantification was possible thank to a chromatographic peak significantly above the detection limit. The C_1-C_5 products detected for the four fuels are carbon monoxide, carbon dioxide, C_1-C_5 hydrocarbons (HC), i.e. methane, ethane, ethylene, acetylene, propene, propyne, allene, 1-butene (not for p-xylene), 1,3-butadiene, 1,3-cyclopentadiene, 1,3-pentadiene (not for toluene and p-xylene), cyclopentene, as well as C_2-C_4 oxygenated species, i.e. acetaldehyde, acrolein, acetone, furan, methacrolein (not for toluene and p-xylene). Formaldehyde was not found. The C_{5+} products detected for the four fuels are benzene, toluene, ethylbenzene, styrene (styrene could not be quantified in the case of o-xylene because its GC peak was too close of that of the fuel), indene, phenol, benzaldehyde and 1,3-benzodioxole (not detected with m-xylene). The related isomers of methylbenzaldehyde, methylstyrene, and methylethylbenzene are detected for each xylene isomer. Phenyloxirane, 2-hydroxybenzaldehyde, o-cresol, benzofuran and 2,3-dihydrobenzofuran are only seen with toluene and o-xylene. o-Xylene, as a product, naphthalene, 1-methylnaphthlene, biphenyl, bibenzyl and cinnamaldehyde are only detected with toluene. m-Cresol was only seen with m-xylene. Phthalan is a product specific to o-xylene oxidation as it will be discussed further in the text. Table S2 also gives the boiling point and melting points of the C_{5+} products. The results further described indicate that our on-line analysis GC method significantly underestimate the formation of oxygenated aromatics with a melting point above 300 K, such as phenol, o- and p-cresol and hydroxybenzaldehyde, which are certainly the most subject to condensation.

All the measured compound mole fractions are provided in an excel spreadsheet in Supplementary Material, together with a list of the structures of the C_{5+} species. The carbon atom balances for the 12 series of experiments are displayed in Tables S2 and S3. Since H_2, H_2O and H_2O_2 were not quantified, no H- or O-atom balance can be provided. Except for a very few experiments, the obtained material balance is between 85 and 115% outside of the temperature range where oscillations were observed, as described hereafter.

3. Kinetic model development

With the aim of modelling the combustion chemistry of surrogates of the aromatic compounds present in biofuels derived from lignin, a new detailed kinetic model named COLIBRI (COmbustion of LIgnin derived Biofuel for Research and Innovation) was developed. This model, provided in Supplementary Material under the CHEMKIN format together with the used nomenclature, includes 463 species and 2836 reactions and combines:

• the Galway C_0-C_3 reaction base [32] for its precision and its efficiency for computing laminar burning velocities,

• the C_{4+} part of the toluene model of Yuan *et al.* [29], which includes reactions of many monoaromatic compounds, such as phenol, benzaldehyde, benzylalcohol, styrene, ethylbenzene, benzofuran and cresol, without separating the isomers, for its accuracy in predicting results for toluene oxidation in all types of reactors, especially JSR,

• the xylene submechanism of Kukkadapu *et al.* [14], which considers the same chemistry for m- and p-xylenes (the two fuels are undifferentiated in the model), as well as low-temperature oxidation pathways for o-xylene,

• the anisole submechanism of Buttgen *et al.* [33] completed by that of Wagnon *et al.* [34] for the reactions of ethylphenol and methylanisole, which is a molecule of interest of our future work, but which helped modelling the formation of 2,3-dihydrobenzofuran in the present study,

• the guaiacol submechanism of Nowakowska *et al.* [35], which is another molecule of interest of our future work.

The Galway C_0-C_3 reaction base [32] was used without any change. Amongst the C_4 reactions considered by Yuan *et al.* [29], only those involved in the aromatic growth and decomposition were kept. The few changes considered in COLIBRI compared to the initial mechanisms are listed in a dedicated spreadsheet Supplementary Material. The thermochemical and transport data of each species are taken from the detailed kinetic model, where the reactions involving the species was first considered, i.e. the thermochemistry of C_0-C_3 species is taken from the model of Burke *et al.* [32], the thermochemistry of small aromatics and PAHs are taken from the model of Yuan *et al.* [29], the thermochemistry of species involved in the xylene submechanisms are taken from the model of Kukkadapu *et al.* [14].

In order to well reproduce the formation of benzofuran and 2,3-dihydrobenzofuran for xylenes, compared to the submechanism of Kukkadapu *et al.* [14], the o- and m/p- isomers of methylbenzaldehyde, methylbenzoyl radical, methylphenyl radical, cresoxy radicals and methylanisole, are distinguished (delumped) in the model as well as the species and radicals linked to them. Indeed, the closure of the second ring is only possible with the ring substituents in ortho position.

As a minor pathway leading to 2,3-dihydrobenzofuran, the mechanism of 2-ethylphenol of Wagnon *et al.* [34] is considered. In addition, the combination of cresoxy and methyl

radicals to yield methylanisole and the cyclisation of the radical obtained from methylanisole by H-abstractions, as well as the H-elimination yielding 2,3-dihydrobenzofuran and reactions consuming 2,3-dihydrobenzofuran were added with rate constants taken from Wagnon *et al*. [34].

In the same way, in order to well reproduce the formation of indene for xylenes, compared to the submechanism of Kukkadapu *et al.* [14], the model COLIBRI distinguishes the isomers of methylethylbenzene, methylstyrene, and their derived radicals and species. In this case, indene is formed from the metatheses on the methyl group of methylstyrene followed by the closure of the second ring. The fact that delumped isomers are considered for all these species leads to an increase of the model of about 200 reactions.

In order to capture the formation of 1,3-benzodioxole, a product experimentally quantified in notable amount, the reaction of addition of phenoxy radical to formaldehyde, followed by a cyclization with H-elimination of the obtained radical, was proposed. The used rate constant for the addition of phenoxy radical to formaldehyde was taken by analogy to that of the addition of CH_3O radical to formaldehyde as proposed by Burke *et al.* [32]; the rate constant of the cyclization yielding 1,3-benzodioxole was taken by analogy to the ipso addition of OH on benzene to mimic a possible ipso addition by RO• radical.

Table 2: Validation targets considered for testing the COLIBRI model using literature data. In flame studies, the indicated temperature is that of fresh gas.

Target	Exp. set-up	Fuel	T (K)	P (atm)	φ	n° Fig.	Ref.
IDT	Shock tube	Toluene	1350-1800	2-8	0.33-1.95	S8	[36]
			1600-1850	1.7-4.5	0.5-1.5	S9	[5]
			1390-1750	1.1	0.5-1.5	S10	[37]
			1020-1400	10-62	0.25-1	S11	[7]
		p-Xylene	1450-1760	1.2	0.5-1.5	S39	[21]
			1050-1400	9-43	0.5-1	S40	[9]
		m-Xylene	1000-1400	9-42	0.5-1	S40	[9]
		o-Xylene	1000-1400	11-44	0.5-1	S40	[9]
			1400-1830	1	0.5-2	S39	[23]
	RCM	Toluene	940-1100	23-45	0.5-1	S12	[14]
		o-Xylene	840-990	24-47	0.5-1	S41	[14]
LBV	Bomb	Toluene	353	1-5	0.7-1.7	S25-S26	[38]
			358-423	1-20	0.6-1.5	S25-S26	[39]
			393-433	1	0.7-1.5	S25	[40]
			400-450	1-3	0.6-1.5	S25-S26	[41]
			450	3	0.8-1.4	S26	[42]
		m-Xylene	450	3	0.8-1.4	S52	[42]
		o-Xylene	353	1-2	0.7-1.5	S52	[38]
	Counterflow	Toluene	298	1	0.7-1.3	S25	[43–
			353	1	0.7-1.5	S25	45]
			400-470	1	0.7-1.4	S25	[46]
			400	1-3	0.7-1.4	S25-26	[47,48]
			403	1	0.7-1.4	S25	[49]
		p-Xylene	353	1	0.7-1.5	S52	[50]
		m-Xylene	353	1	0.7-1.5	S52	[46]
		o-Xylene	353	1	0.7-1.5	S52	[46]
							[46]
	Flat flame burner	Toluene	298	1	0.8-1.3	S25	[51]
			298-358	1	0.7-1.3	S25	[52]
			298-398	1	0.55-1.55	S25	[53]
		p-Xylene	328-353	1	0.7-1.4	S52	[54]
	Bunsen burner	Toluene	400	1	0.6-1.5	S25	[55]
			423	1	0.6-1.3	S25	[56]
Product profiles	Shock tube	Toluene	1200-1900	10	Pyrolysis	S13	[57]
			1200-1500	20-53	1-5	S14	[58]
			1100-1900	22-50	Pyrolysis	S15	[59]
		p-Xylene	1090-1670	19-22	Pyrolysis	S43	[60]
		m-Xylene	900-1630	24-58	0.5-2.35	S42	[10]
			1140-1650	19-22	Pyrolysis	S43	[60]
		o-Xylene	1150-1650	19-22	Pyrolysis	S43	[60]
	JSR	Toluene	1000-1400	1	0.5-1.5	S2-S4	[24]
			950-1200	10	0.5-1.5	S5-S7	[29]
		p-Xylene	1050-1400	1	0.5-1.5	S27-S29	[21]
		m-Xylene	1050-1400	1	0.5-1.5	S30-S32	[22]
		o-Xylene	1050-1350	1	0.5-1.5	S33-S35	[23]
			800-1200	10	0.5-2	S36-S38	[27]
	Flow reactor	Toluene	1100-1600	0.04-1	Pyrolysis	S16-19	[29]
		o-Xylene	1050-1600	0.04-1	Pyrolysis	S44-S45	[27]
	Laminar flame	Toluene	300	0.04	0.75-1.75	S20-24	[61]
		p-Xylene	300	0.04	0.75-1.79	S49-51	[28]
		o-Xylene	300	0.04	0.75-1.79	S46-48	[62]

All simulations described in this work were performed using the CHEMKIN software [63]. For JSR data, simulations were performed using the transient solver of the PSR module over an integration time of 100 s to allow the steady state to be perfectly established. As it is shown in SM (Figures S2 to S52), this model reasonably predicts many kinetic data of literature on Ignition Delay Times (IDT), species profiles and Laminar Burning Velocities (LBV) found for the four considered reactants.

Table 2 summarizes the validations targets, which are presented in SM. The validation of this model for oxygenated aromatics, e.g. anisole and guaiacol, will be presented in future papers.

4. Experimental results and comparison with modelling

The experiments for the four fuels of interest in this study were performed under isothermal conditions, at temperatures from 600 to 1200 K, a pressure of 1.07 bar, a residence time of 2 s, an initial fuel mole fraction of 0.005, and equivalence ratios of 0.5, 1 and 2. Figures displaying the experimental and predicted temperature evolutions of the mole fractions of fuel, O_2, and all the products quantified with a mole fraction above 5 ppm under at least an experimental condition, are provided in SM (Figures S53 to S61) for the three considered equivalence ratios. An example of the repeatability is presented in Figure S62 in the case of toluene.

In order to discuss the reactivity of the four fuels, the experimental and simulated mole fractions of these fuels and that of the non-oxygenated aromatic products common to the three isomers of xylene, and when possible, toluene, are displayed in Figure 1 for an equivalence ratio of 1; in Figures 1 to 5, the error bars are the errors on the GC analyses. Only CO_2 mole fraction is drawn for φ = 0.5 to show a maximum of formation, since it is the product, for which a decrease of the equivalence ratio increases the most significantly

its production; moreover, important experimental oscillations are encountered for CO_2 at φ = 1. Figures 2 to 4 present the experimental and simulated mole fractions of the oxygenated aromatic and C_1-C_5 products common to the three xylenes. For sake of figure readability, error bars are only displayed for o-xylene.

As it was already discussed in previous JSR oxidation studies, e.g. for the oxidation of methane [64] or acetone [31], the experimental disordered evolution of some mole fraction profiles observed above 1050 are due to oscillations; this oscillating behavior is also reproduced by the COLIBRI model when simulations were performed under transient conditions. Under the conditions where oscillations are numerically encountered, the transient calculation time is longer by a factor of about 100 than without oscillation, for which it is very fast. An example of the predicted oscillations is given in Figure S63 in SM, which shows well a periodic behavior for the time evolution of the mole fraction of the fuel, CO and toluene as a product. To experimentally record such a behavior, a mass spectrometer needs to be used instead of GC as in our previous studies [31,64]; but here it was outside the scope of our work. However, in Figures 1 to 4 and S53 to S61, the results above 1050 K are shown to illustrate this phenomenon, which is not so experimentally apparent, since the GC analysis operates a kind of averaging of the species mole fraction, but which explains why the agreement between experimental values and simulated ones obtained at the end of the integration time is often deteriorated. This phenomenon particularly affects the mole fraction of CO and CO_2, the major products in this temperature range, but less that of the products specific to the oxidation of the studied aromatic compounds.

Figure 1 well shows that, as assumed by Kukkadapu *et al.* [14], p- and m-xylenes have a similar reactivity close to that of toluene and that of o-xylene is significantly more

reactive, since it starts to react at a temperature of about 100 K lower than the 3 other fuels. This difference of reactivity is very well reproduced by simulations using the COLIBRI model. The promoting effect of decreasing the equivalence ratio is also satisfactory reproduced by the model (see Figure S53); only the model underpredicts the O_2 consumption of m- and p-xylenes between 875 and 950 K for φ = 0.5, while the agreement is satisfactory under the same conditions for toluene and o-xylene.

The highest reactivity of o-xylene is confirmed by the profiles of C_1-C_5 products displayed in Figures 3 and 4, for which the highest mole fractions below 1000 K are always obtained with it. Toluene, p- and m-xylenes exhibit a similar formation of CO, a compound indicative of the overall reactivity.

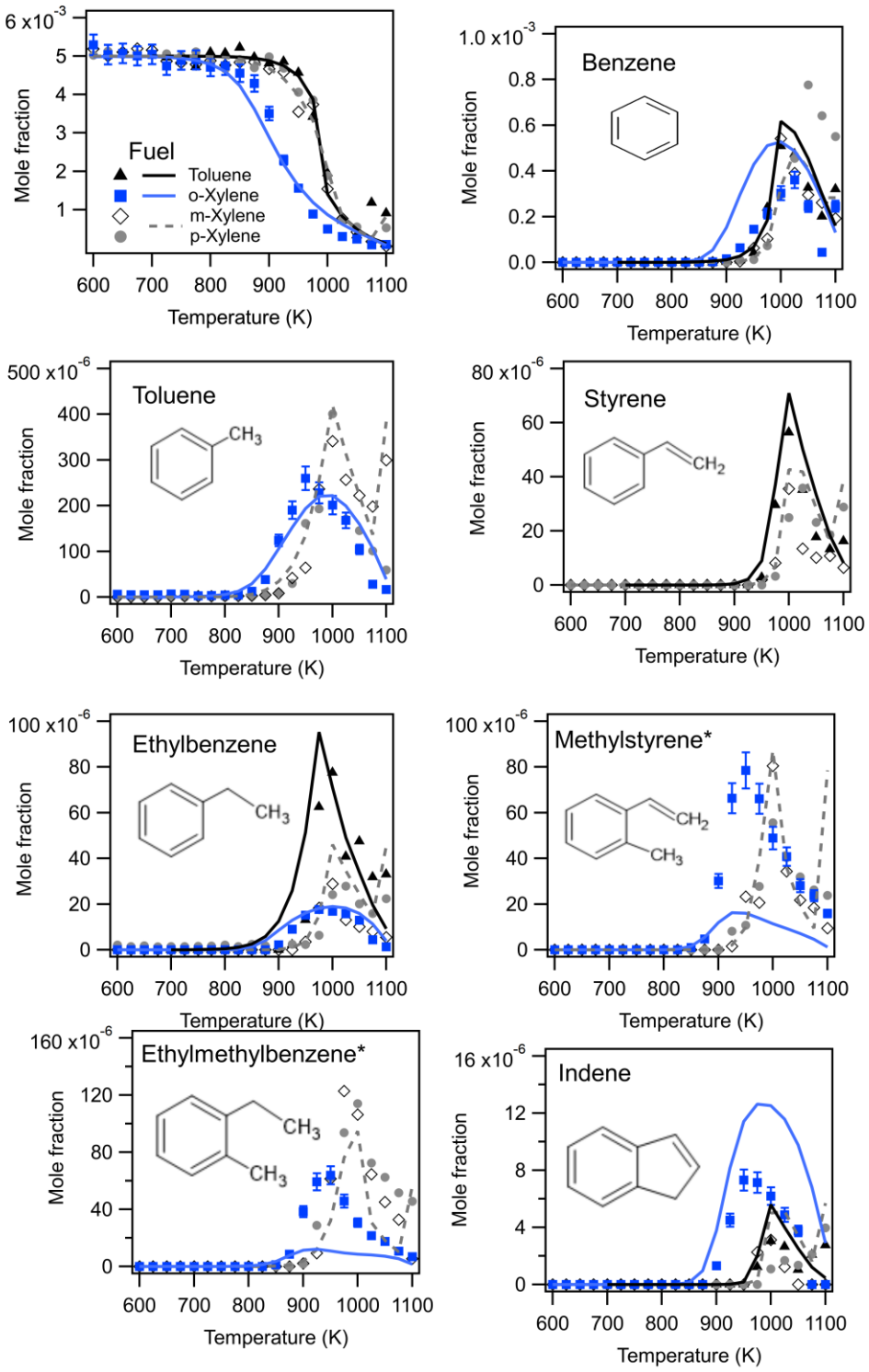

Figure 1: Experimental and predicted mole fractions as function of temperature of the four fuels and of the non-oxygenated aromatic products common to the three isomers of xylene, and when possible, toluene, for an equivalence ratio of 1. *The drawn structure corresponds to the isomer formed from o-xylene.

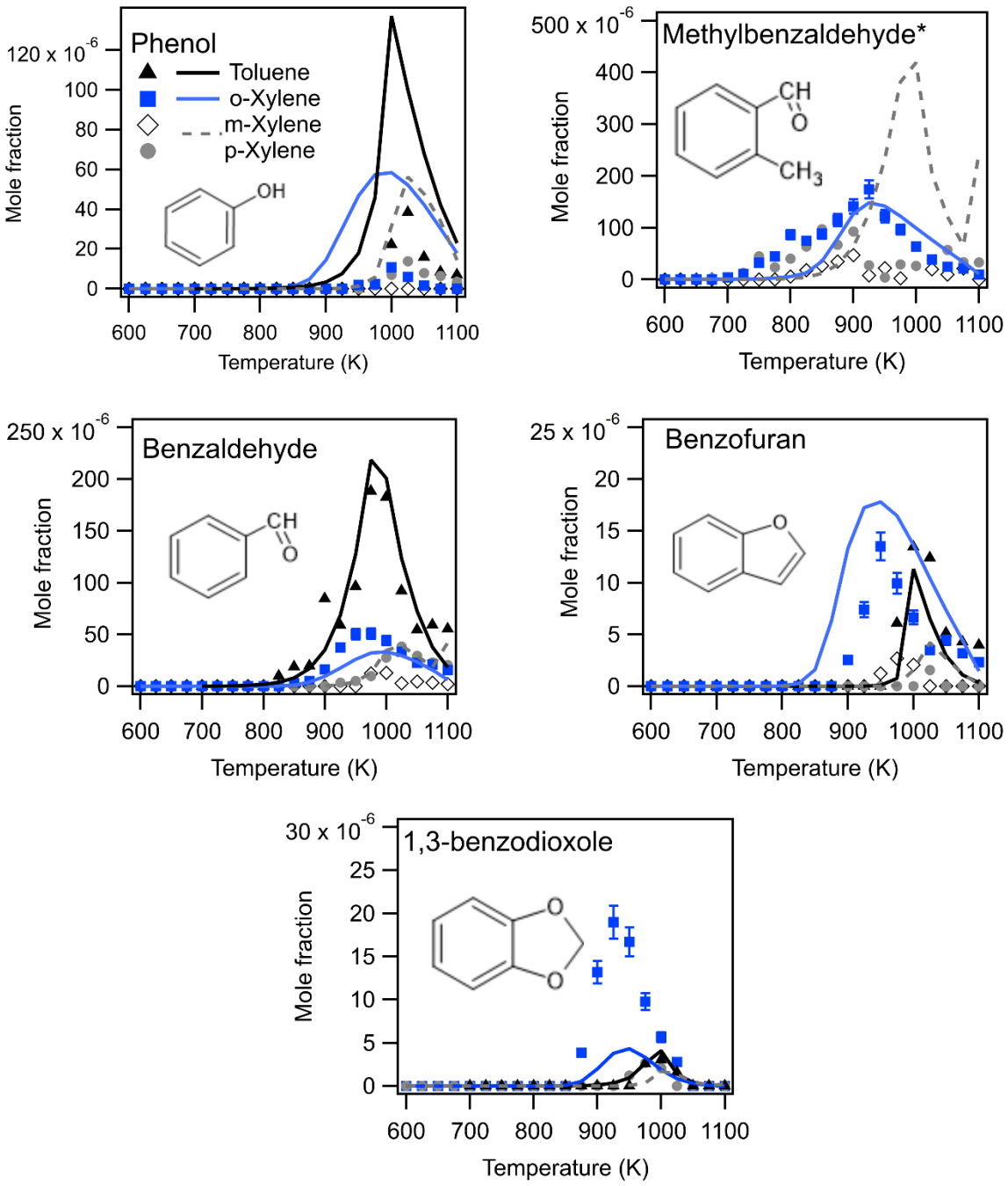

Figure 2: Experimental and predicted mole fractions as function of temperature of the oxygenated products common to at least two isomers of xylene, and when possible, toluene, for an equivalence ratio of 1. Error bars are only displayed for o-xylene. *The drawn structure corresponds to the isomer formed from o-xylene.

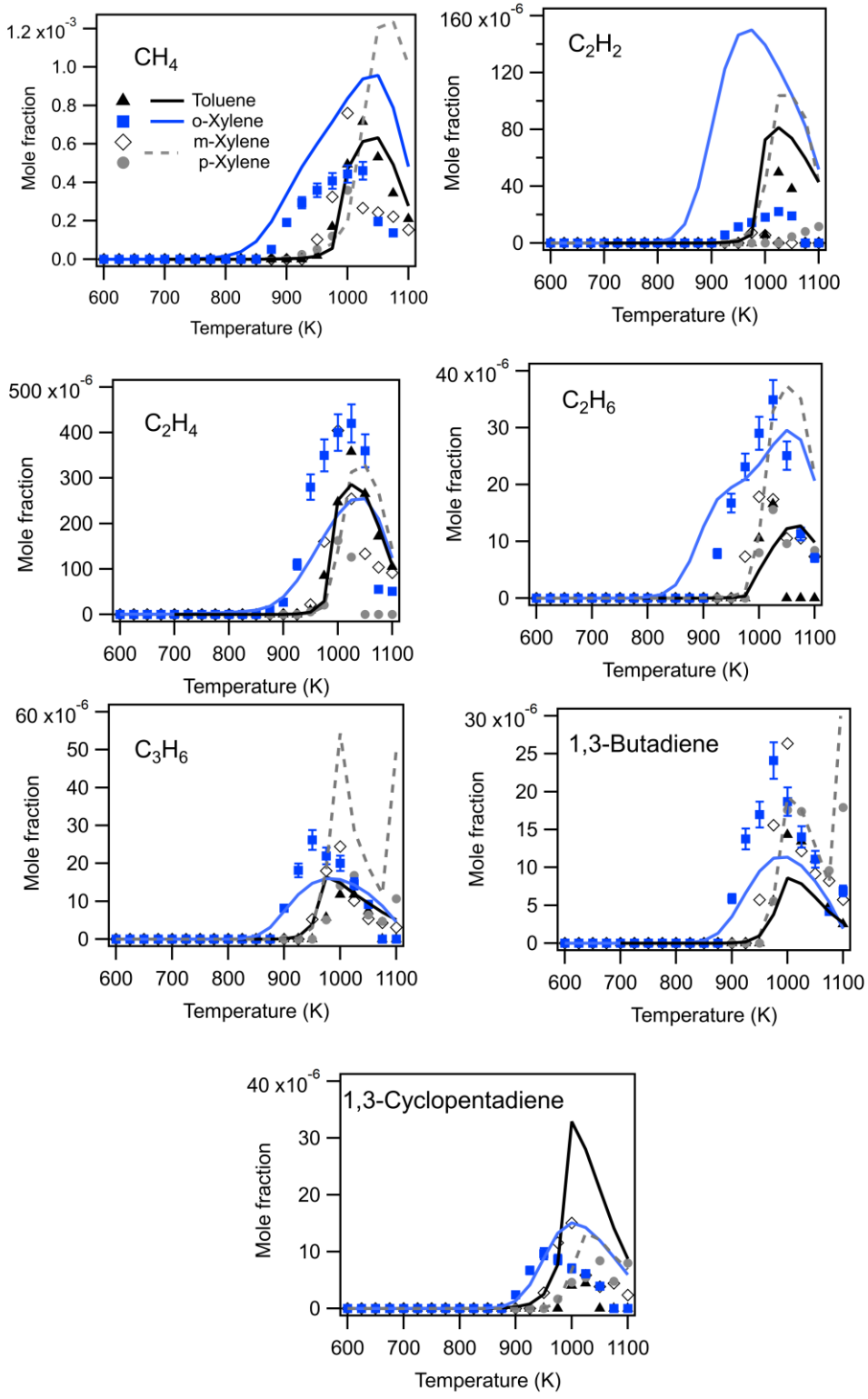

Figure 3: Experimental and predicted mole fractions as function of temperature of the non-oxygenated C_1-C_5 products common to the four fuels (φ = 1). Error bars are only displayed for o-xylene.

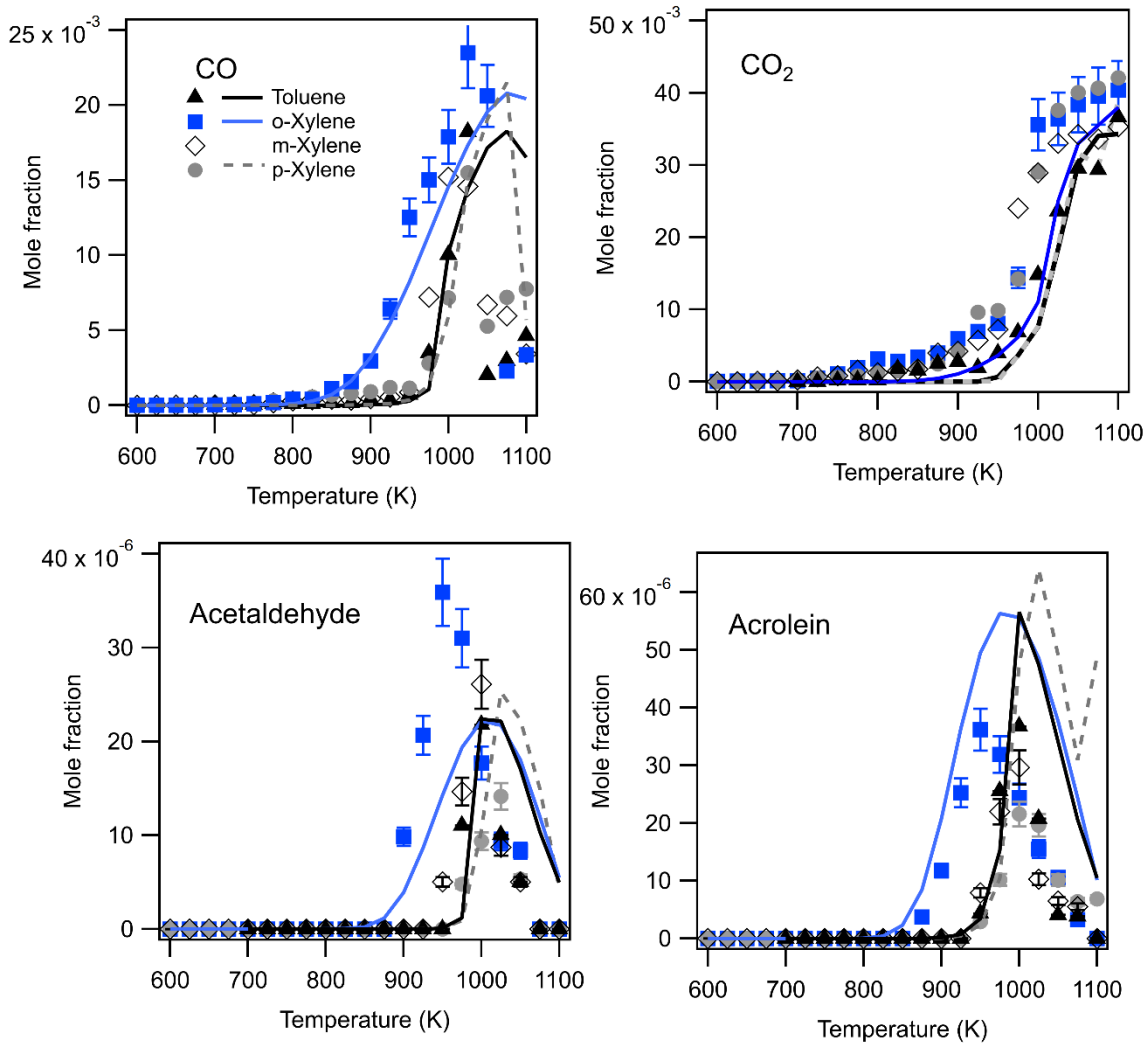

Figure 4: Experimental and predicted temperature mole fractions as function of temperature of the oxygenated C_2-C_4 products common to the four fuels (φ = 0.5 for CO_2, 1 for the other products). Error bars are only displayed for o-xylene.

As it is shown in Figure 4, the formation of CO_2 is also reasonably predicted by the model for the four fuels. However, an unexplained formation of up to 10,000 ppm is observed from 750 K for the four fuels. This formation, which was observed by GC with both FID-methanizer and by TCD and using two separate JSR set-ups for toluene, but never in absence of fuel, does not depend on the equivalence ratio. It has been hypothesized that undetected cyclic ketones, which are predicted to be formed in significant amounts (see discussion in part 5) might be converted to CO_2 in the transfer line, but their predicted

formation at 800 K is too low for m/p-xylenes and toluene. Whatever its origin, this CO_2 formation does not seem to influence the results obtained for the other species.

Despite the close temperature evolutions of the mole fraction of fuel, CO, CO_2, ethylene, 1,3-butadiene, toluene, styrene, benzaldehyde, and ethane, possible differences are encountered between m- and p-xylene in the formation of some products. A larger formation of benzene by about a factor of 1.5 is observed with p-xylene, while m-xylene yields more propene, 1,3-butadiene 1,3-cyclopentadiene and benzofuran. This might indicate some slight differences of chemistry between both compounds.

The model leads to a reasonable agreement for most of the quantified species, for the three considered equivalence ratios (see Figures S53 to S60 in SM). For o-xylene, the predicted formation of o-ethylmethylbenzene and o-methylstyrene is significantly lower than the experimental ones, especially in stoichiometric and rich mixtures. The deviation is still worse for phenol with an overprediction by a factor of about four for toluene and at least of 10 for xylenes; phenol is not even detected for m-xylene. This might be due to condensation of this molecule, which is solid at room temperature and has a boiling point of 455 K. Moreover, the lack of data on the phenol kinetics, especially at temperatures below 1050 K [3], does not facilitate its accurate modelling.

While the prediction of methylbenzaldehyde is reasonable for o-xylene, a very large overprediction is observed for m/p-xylenes. For the four methylated benzenes, the model significantly overpredicts the formation of acetylene; over 1000 K; methane is overpredicted for m/p-xylene and 1,3-cyclopentadiene for toluene.

Thanks to the new channel from phenoxy radicals for the formation of this di-oxygenated compound, the formation of 1,3-benzodioxole (see Figure 2) is well reproduced by

COLIBRI for toluene and p-xylene oxidation; however, its formation for o-xylene is underpredicted by a factor of four indicating that there is still a reaction pathway missing.

Figure 5 concerns the products specific to o-xylene amongst xylene reactants and displays the temperature evolution of their mole fractions for the three used equivalence ratios, 0.5, 1 and 2. These products are 2-hydroxybenzaldehyde, 2,3-dihydrobenzofuran and phthalan. 2-Hydroxybenzaldehyde and 2,3-dihydrobenzofuran were also quantified in very low amounts during toluene oxidation, as it is also the case for naphthalene, and stilbene. Because the chemistry of toluene fuel is better known, figures concerning the formation of these five products from toluene are only displayed in SM (Figure S55). Amongst those products, only naphthalene is reasonably simulated.

Figure 5 shows that while 2-hydroxybenzaldehyde and 2,3-dihydrobenzofuran are only produced at temperatures above 800 K and can also be detected for toluene, phthalan is a product specific to o-xylene, with a noticeable mole fraction between 600 K and 700 K for □ equal 0.5, together with a negative temperature coefficient (NTC) behavior. This NTC behavior is indicative of the occurrence of low-temperature chemistry involving addition to oxygen as it was proposed by Roubaud *et al.* [13].

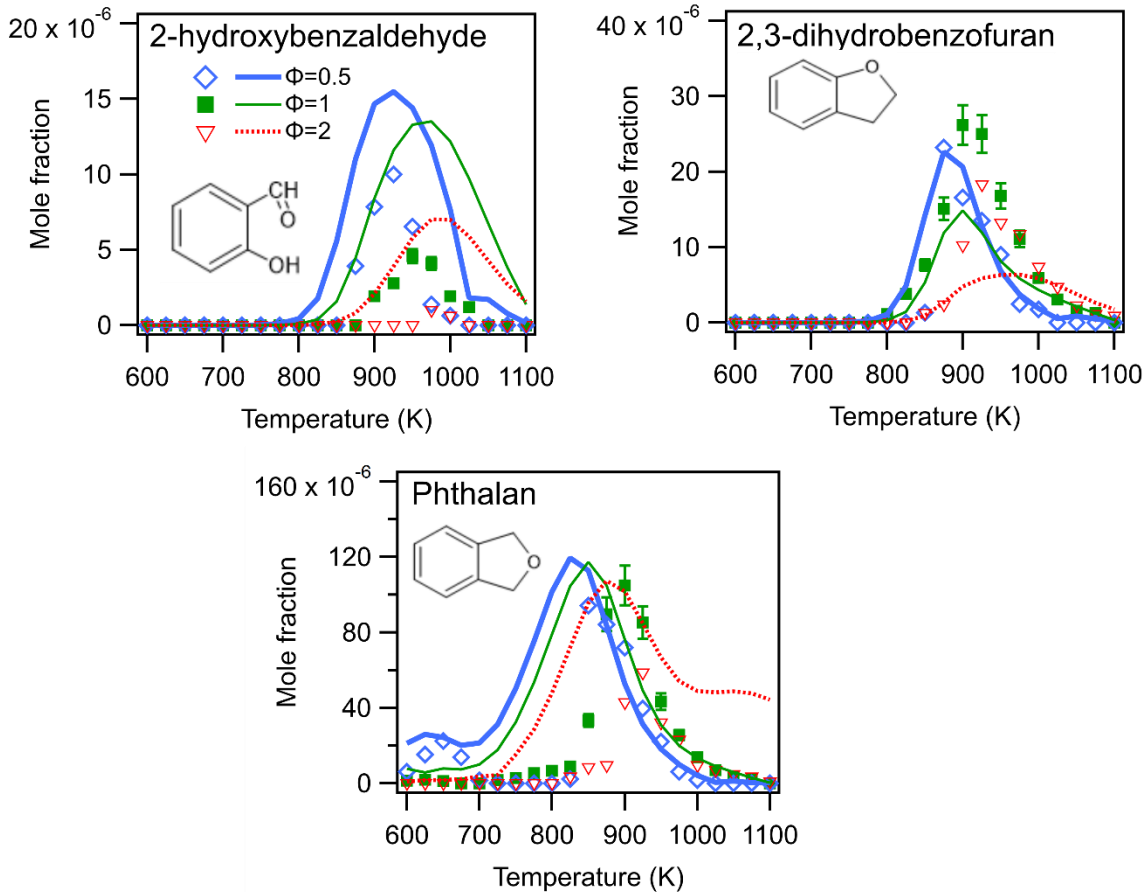

Figure 5: Experimental and predicted temperature mole fractions as function of temperature of the products only quantified for o-xylene amongst xylene isomers. Error bars are only displayed for φ = 1.

As indicated by Figure 5, during o-xylene oxidation, simulations using the COLIBRI model allow reasonably capturing the temperature profile of phthalan and 2,3-dihydobenzofuran at the three φ. Concerning phthalan, the model simulates well the experimentally observed NTC behavior at φ = 0.5; to obtain the present agreement, the A-factor of the H-abstraction by OH radicals was divided by a factor of three compared to the model of Kukkadapu et al. [14]. The prediction of the 2,3-dihydrobenzofuran profile was significantly improved by considering the reactions proposed by Wagnon et al. [34] for methylanisole. The temperature of the maximum mole fraction of

2-hydroxybenzaldehyde is also reasonably predicted; however, the experimental mole fractions are underpredicted by 50% at φ = 0.5 and a factor of 6 for φ = 2.

Several products, such as formaldehyde, cyclopentadienone and quinonemethide, are numerically predicted in significant amounts (~100 ppm), but were not detected experimentally due to not well-identified reasons (condensation, catalytic decomposition…). Their predicted temperature evolution at φ = 1 is given in Figure S64. For formaldehyde, its maximum computed mole fraction at φ = 1 is 9.10^{-5} for toluene, $1{,}5.10^{-4}$ for p-xylene and $1{,}4.10^{-4}$ for o-xylene.

Note that by using a higher residence time (2 s) compared to past studies [21–24,27,29] (below 1 s) allowed obtaining a significant reactivity at lower temperature for the four fuels (see Figure S65), and consequently better analyzing the products yielded at lower temperature, such as phenol, 2.3-dihydrobenzofuran, o-cresol, quantifying new species like 1,3-benzodioxole and putting in evidence the NTC behavior of phthalan around 650 K.

5. Kinetic analyses

Since an overall acceptable agreement was obtained between the experimental results and modelling, the COLIBRI model was used to perform kinetic analyses in order to better understand the chemical pathways involved in the consumption of the four methylated reactants and in the formation of the products displayed in Figures 1 to 5. First, the pathways involved in the high-temperature oxidation of the four methylated benzenes are compared, afterward the low-temperature chemistry of o-xylene is detailed.

5.1.High-temperature chemistry of the toluene and xylene isomers

Figure 6 displays flow rate analyses performed for toluene (at 990 K), o-xylene (at 915 K) and p-xylene (at 995 K); these temperatures correspond to a fuel conversion of 50% under the condition of Figure 1. In this Figure, the numbers are the % of flow rate of the reacting species; apart from those of the o-methylbenzyl radical, only the channels corresponding to a fuel consumption above 5% are displayed. In addition, R• are mainly OH•, H•, •O•, and CH_3• radicals, dotted lines indicate steps involving several reactions of the model, and compounds in a box are quantified aromatic products.

Figure 6 indicates that the three fuels are consumed by three main channels: the abstractions of a benzylic H-atom, which is the major pathway, the abstractions of a phenylic H-atom, and the ipso-addition of an H• atom removing a methyl group. With the used rate constants, which are taken from combined experimental and theoretical work of Seta et al. [65], the H-abstractions from toluene by OH radicals account for 59%% of the formation of benzyl radicals and for 86% of that of methylphenyl ones. The fact that the enthalpy of formation of the benzyl radical is 20 kcal/mol lower than that of the methylphenyl one makes a higher number of radical types to be involved in the abstraction of a benzylic H-atom, e.g. H and O atoms, OH, CH_3, HCO, and phenoxy radicals, while it is mostly OH radicals for that of a phenylic H-atom. The addition of •O• atom to the fuel is also notable for toluene and leads to cresol, a product quantified in this study, but with a maximum mole fraction below 5 ppm. This channel is also considered for xylenes, but accounts for less than 5% of fuel consumption.

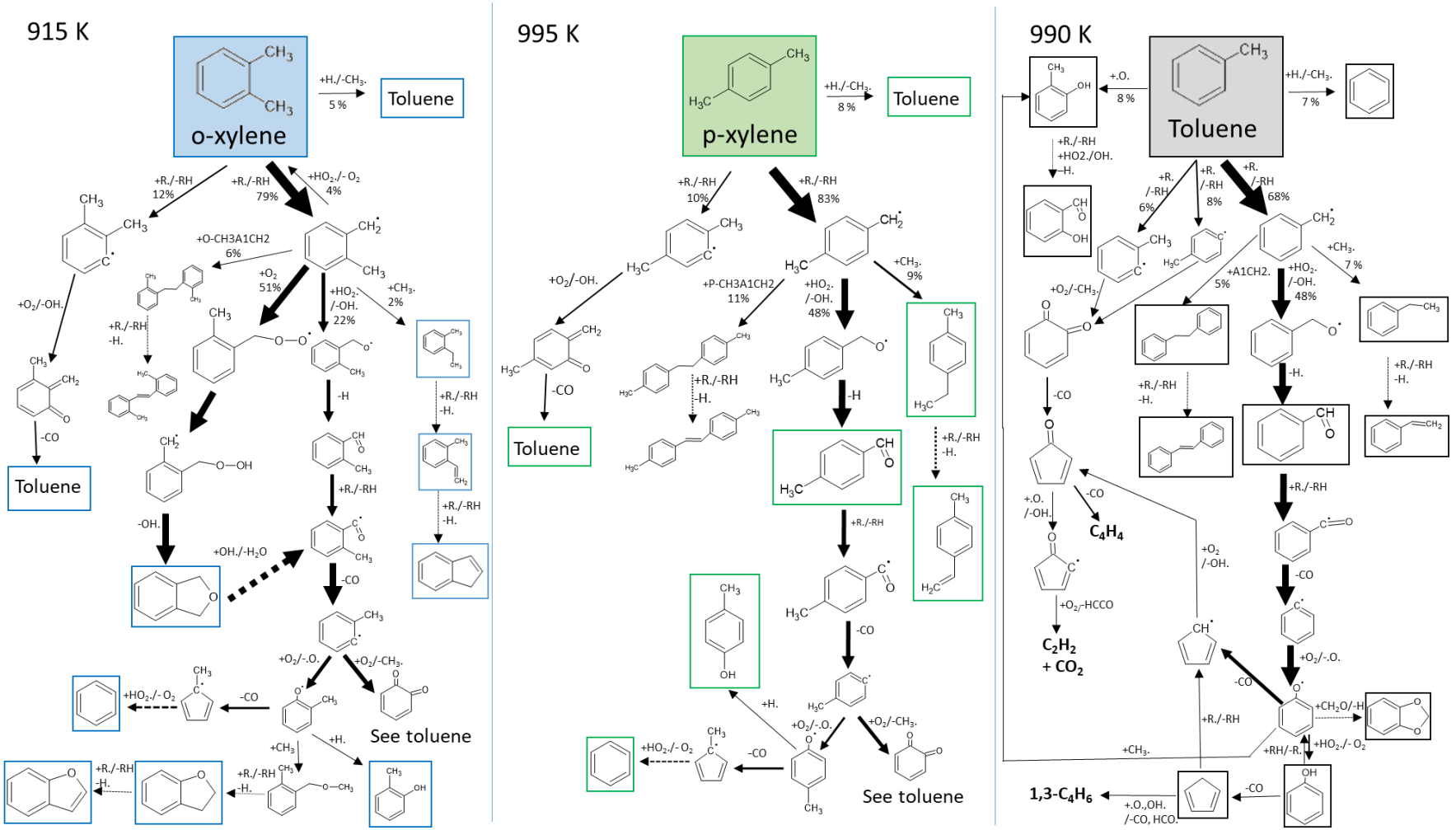

Figure 6: Flow-rate analyses during the oxidation of toluene, o-xylene, and p-xylene (same as m-xylene). Fuel conversion of 50%, φ = 1.

The ipso-addition of an H• atom removing a methyl group leads to benzene from toluene for about a third of its formation, and to toluene from each xylene; both products were quantified during xylene oxidation (see Figure 1). In xylene oxidation, toluene is readily consumed when produced involving the same pathways as when it is the reactant, while it is not the case for benzene.

5.1.a. *Reactions of the phenylic radicals*

In the case of toluene as reactant, the phenylic radicals obtained by metatheses reacts with O_2 and yields mainly o-benzoquinone and methyl radicals, the self-combination of which yields ethane. The channel involving the formation of C_2H_5• radicals obtained by H-abstraction from ethane is the main pathway towards ethylene. Ethane and ethylene were quantified for the four fuels, in large amounts for C_2H_4 (maximum mole fraction about 400 ppm for o-xylene at 1025 K), and their formation was reasonably predicted (see Figure 3).

Despite o-benzoquinone was not be detected in this study, the production of o-benzoquinone is the pathway with the largest flow rate amongst those proposed by Da Silva *et al.* [66] and considered in the COLIBRI model; the branching reaction yielding an •O• atom and a cresoxy radical is about twice less important. Afterward, o-benzoquinone eliminates CO to produce cyclopentadienone as proposed for p-benzoquinone by Alzueta *et al.* [67].

Cyclopentadienone (not detected here, despite a predicted mole fraction up-to $1x10^{-4}$) can react by molecular CO elimination yielding vinylacetylene, C_4H_4, or to a lesser extent by H-abstractions to give to a radical that reacts with O_2 to produce to CO_2, C_2H_2 and •HCCO radical, a precursor of CO and CO_2. This globalized reaction is the main pathway leading

to acetylene and the large uncertainties on its kinetics might explained the large deviations between experiments and modelling indicated by Figure 3.

C_4H_4 was not detected in our study, but its reactions are the source of other quantified products. The reaction of C_4H_4 with OH radicals yields allyl radicals, which give propene by reaction with H-donors (e.g. fuels, C_3H_6, $\bullet HO_2$ radical…), and produce acrolein by reaction with $\bullet HO_2$ radicals; further reactions of acrolein are at the origin of the formation of acetaldehyde. As shown in Figures 3 and 4, propene, acrolein and acetaldehyde were quantified in this study in notable amounts and are reasonably predicted by the COLIBRI model.

For the reaction with O_2 of the phenylic radicals obtained from o- and p-xylenes, as indicated in Figure 6, Kukkadapu *et al.* [14] considered only the formation of methyl o- and p-quinone methides, based on a pathway also proposed by Da Silva *et al.* [66] for toluene involving an O_2 addition, an H-transfer and an OH elimination. This molecule, which was not detected despite a predicted mole fraction up to $3x10^{-4}$, further decomposes in CO and toluene. In order to consider in more details these reactions, it might be interesting to apply to xylene isomers the theoretical analysis made by Da Silva *et al.* [66] for toluene.

During xylene oxidation, methylphenyl radicals are produced in large amounts as intermediates derived from methylbenzaldehyde as described hereafter. Under these conditions, the significant reactions consuming methylphenyl radicals are not only those towards o-benzoquinone as during toluene oxidation. For the three xylene isomers, the formation of cresoxy radicals accounts for more than 5% of the fuel consumption, with their decomposition being responsible of a second way of formation of benzene through a C_5 reaction pathway occurring after a CO elimination. This explains the large amounts

of benzene experimentally quantified. Further theoretical calculations for the decomposition of cresoxy and methylcyclopentadienyl radicals might be useful to understand why the formation of benzene seems to be favored for p-xylene.

The flow rate of another channel from the three isomers of cresoxy radical is also notable, the formation of cresol by reactions with H-atoms. Only m-cresol was quantified during m-xylene oxidation (see Figure S59). The fact that cresol is not detected for o-/p-xylene oxidation is most probably due to condensation in the transfer line towards GC and also to the lack of data on their kinetics [3] as in the case of phenol. Note that o- and p-cresols are solid at room temperature with melting points of 304 and 307 K, respectively. The fact that m-cresol has a lower melting point, 284 K, might explain why is it the only one detected in this study.

In the special case of o-xylene a last channel from o-cresoxy radicals should be considered: its combination with a methyl radical yielding methylanisole (not experimentally detected). The radical produced from methylanisole by H-abstractions, can cyclize and eliminate a H• atom to yields 2,3-dihydrobenzofuran, which at its turn leads to benzofuran. These channels explain why benzofuran and 2,3-dihydrobenzofuran were experimentally quantified during o-xylene oxidation in notable amounts and why they are reasonably predicted by the model (see Figures 2 and 5, respectively).

As described hereafter, phenyl radicals are produced during oxidation of the four considered methylated benzenes. They mostly react by a branching step with O_2 to give a phenoxy radical and a •O• atom. Besides reacting with methyl radicals to yield cresol, which is their main fate, and with the available H-atom donors to produce phenol, phenoxy radicals reacts by CO elimination to give the cyclopentadienyl radicals. Figure 6

also indicates that a small part of phenoxy radicals reacts with CH_2O to yield 1,3-benzodioxole, a product quantified with toluene, o- and p-xylenes (see Figure 2).

While it is not indicated in Figure 6, because the flow rate is too small, a tiny part of phenoxy radicals also reacts with C_2H_2 to produce benzofuran; this is a minor source of this compound for o-xylene, which is mainly formed from 2,3-dihydrobenzofuran, as herebefore described; but the major source for toluene and m/p-xylenes. As shown in Figure 2, the formation of benzofuran is well predicted by the model for toluene and o-xylene.

Phenol is a product quantified during the oxidation of the four fuels, even if the model does not well predict its mole fraction profiles (see Figure 2) due to previously mentioned condensation issues. Besides giving back phenoxy radicals by H-abstractions, phenol leads, by CO elimination induced by OH radicals, to 1,3-cyclopentadiene, another product quantified for the four fuels (see Figure 3) and reasonably predicted. According to the model used for this flow rate analysis, besides producing 1,3-butadiene by reaction with $\bullet O\bullet$ and $\bullet OH$ radicals, cyclopentadiene yields cyclopentadienyl radicals which mainly react with O_2 to give cyclopentadienone. 1,3-Butadiene was quantified for the four fuels, and its production is reasonably predicted by the model (see Figure 3).

5.1.b. *Reactions of the benzylic radicals*

For the four fuels, a significant part of the resonance stabilized benzylic radicals obtained by H-abstractions reacts by self-combination or by combination with a methyl radical. For toluene, the product of the self-combination of benzyl radicals is bibenzyl, which yields stilbene by H-abstraction followed by H-elimination. These compounds were experimentally observed in this study, but only in trace amounts. As shown in Figure 6, the model predicts analogous pathways for xylenes, but the corresponding products were

not detected, probably because they are too heavy (16 atoms of carbon) and might condensate in the transfer line.

The combination of a benzylic and a methyl radical is at the origin of the formation of ethylbenzene and styrene for toluene and of the respective methylethylbenzene and methylstyrene isomer for each xylene. During xylene oxidation, styrene and ethylbenzene are produced by the secondary oxidation of the produced toluene. These compounds were quantified for the four fuels (see Figure 1) and their primary and secondary formations were satisfactorily predicted. Due to the ortho position of both substituents, during o-xylene oxidation, the radical obtained by abstraction of the benzylic H-atom from methylstyrene can cyclize and after a C-H bond breaking leads to the formation of indene, a compound quantified in significant amounts with o-xylene as it is well-predicted by COLIBRI (see Figure 1). Indene is formed in lower amounts during toluene and m/p-xylene oxidation through a pathway involving cyclopendadienyl radical and C_2H_2.

In the case of toluene and p/m-xylenes, the major consumption pathway of the benzylic radical is its reaction with $\bullet HO_2$ radicals yielding benzaldehyde or p/m-methylbenzaldehyde, respectively, through the formation of a benzoxy or methylbenzoxy radical. The same type of reaction leading to o-methylbenzaldehyde exists also for o-xylene, but it is not the major pathway consuming the benzyl radical, as it will be discussed further. The obtained benzaldehydes react by H-abstractions, with formation of benzoyl and methylbenzoyl radicals, followed by CO elimination yielding phenyl and methylphenyl radicals, respectively. During xylene oxidation, non-substituted benzaldehyde is also produced by the secondary oxidation of the toluene. The formation of benzaldehyde is well predicted during toluene and xylene oxidation; that of methylbenzaldehyde is reasonably predicted during o-xylene oxidation (maximum

experimental mole fraction about 200 ppm), but overpredicted by a factor of more than five for p/m-xylene oxidation (see Figure 2). This might be due to condensation of these two compounds in the transfer line when they are formed in large amounts at the level predicted by the model. This series of reactions is also possible for the benzylic radicals derived from cresol and explains the formation of hydroxybenzaldehyde, a product quantified and reasonably predicted by the model during the oxidation of o-xylene (see Figure 5), but with important deviations for toluene (see Figure S55).

In the case of o-xylene, the major channel consuming the resonance stabilized methylbenzyl radicals is the addition to oxygen, followed by an internal isomerization and the formation of phthalan and OH radicals, see more details in the next section. This additional propagation channel from methylbenzyl radicals competes with the reaction with $\bullet HO_2$ radicals, which starts by a combination, and explains the highest reactivity of o-xylene.

Phthalan readily reacts by H-abstractions with OH radicals to give a radical, which isomerizes to produce a methylbenzoyl radical, a source of cresol, benzene and 2,3-dihydrobenzofuran. As shown in Figure 5, the formation of phthalan is well reproduced by the model above 900 K, but overpredicted between 700 and 900 K.

52. Low-temperature chemistry of o-xylene

Figure 7 displays a flow rate analysis made during the oxidation of o-xylene at 650 K, the temperature corresponding to the maximum of formation of phthalan below 800 K. In this temperature zone, a small formation of CO (25 ppm at 650 K for φ = 0.5) is also experimentally observed, but with no NTC behavior. As shown in Figure 7, o-xylene exhibits a low-temperature chemistry similar to that observed for alkanes and

characterized by the formation of ketohydroperoxides in concurrence with that of cyclic ethers [68].

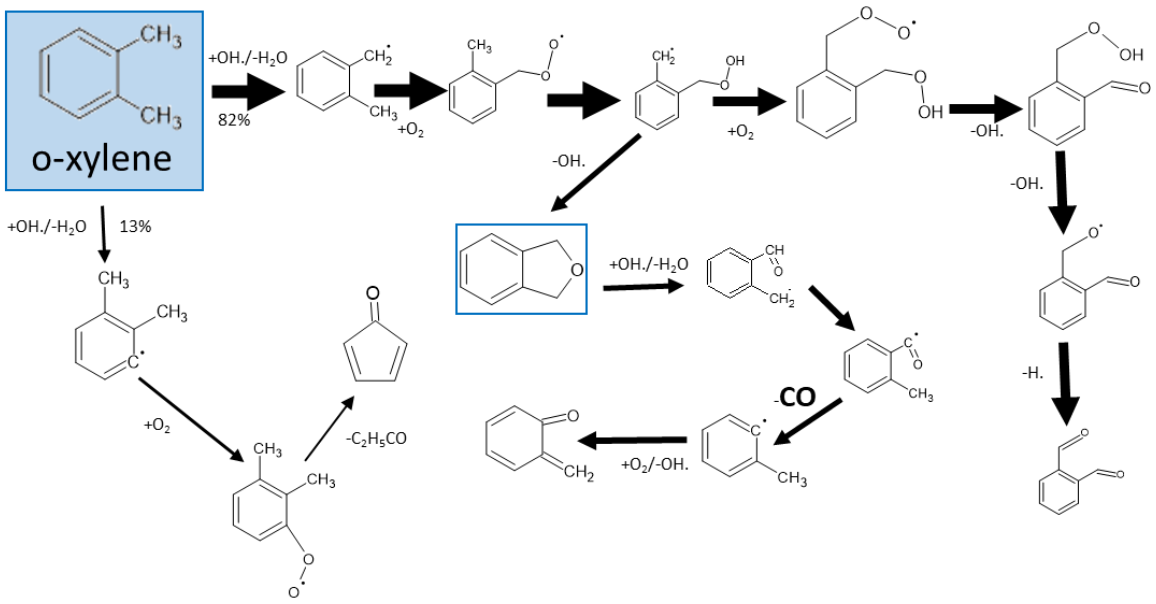

Figure 7: Flow-rate analysis during the oxidation of o-xylene at 650 K.

At 650 K, o-xylene is mainly consumed by H-abstractions, mostly with OH radicals, to give di-methylphenyl and methylbenzyl radicals. Both radicals react mostly by addition to O_2. After the addition to O_2, di-methylphenyl peroxy radicals mainly decompose to yield cyclopentadienone and C_2H_5CO radicals. Thanks to the methyl group in ortho-position, methylbenzyl peroxy radicals isomerize by internal transfer of an H-atom. The obtained • QOOH radicals may either decompose to yield phthalan, as previously described, or add again to O_2 and lead to the ketohydroperoxide drawn in Figure 7. Phthalan reacts by H-abstraction yielding formyl benzyl radicals, which isomerize to give methyl benzoyl radicals, leading by CO-elimination to methylphenyl radicals, which adds to O_2 to finally give o-quinone methide as proposed by Da Silva *et al.* [66] for toluene. The decomposition of the ketohydroperoxide is a branching step involving the formation of an • OH radical and an H• atom and producing an aromatic compound with two aldehyde functions (o-phthaldehyde); neither this last species, nor o-quinone methide was detected in our

study. However, o-phthaldehyde was quantified by Yuan *et al.* [27]. Starting by an H-abstraction of an aldehydic H-atom, o-phthaldehyde yields in a few steps CO and a benzoyl radical and its mole fraction is predicted in our conditions to be below 1 ppm.

Figure 8 displays a sensitivity analysis at 650 K on phthalan mole fraction and confirms the conclusions drawn from Figure 7. The reactions with largest positive sensitivity coefficient are the H-abstractions yielding methylbenzyl radicals, the second addition to O_2, and the formation of the aromatic ketohydroperoxide. These three reactions promote the reactivity, and consequently the formation of phthalan. In contrast, the reactions with largest negative sensitivity coefficient are the H-abstractions yielding dimethylphenyl radicals, which competes with the formation of methylbenzyl radicals, the reverse of the second O_2 addition, the formation of the cyclic ether, and its consumption.

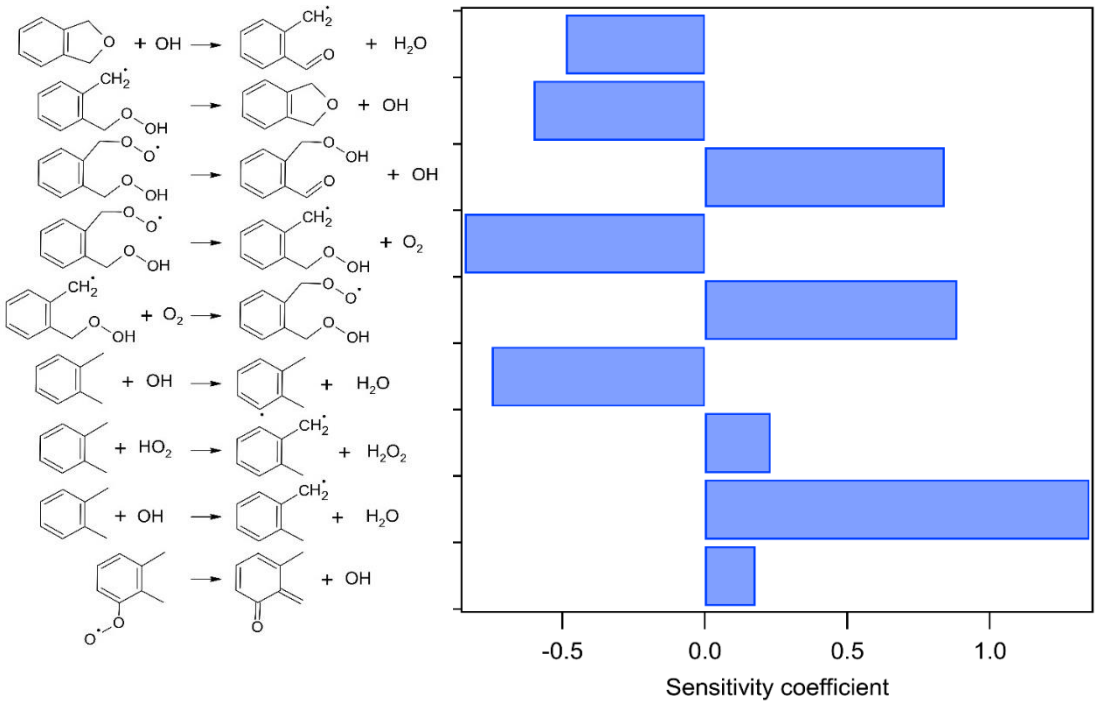

Figure 8: Sensitivity analysis on phthalan mole fraction at 650 K (see Figure S66 in SM for the reactions written as in the model). Only coefficients above 0.15 are displayed.

The reaction forming the cyclic ether from the •QOOH radical has a surprising negative influence on its mole fraction: because it competes with the second O_2 addition leading to the branching step, it inhibits the global reactivity.

6. Conclusion

This paper presents an experimental and modelling comparison of the oxidation of toluene and the three isomers of xylene. Apart from a few products (e.g. benzene), this work confirms the hypothesis made by Kukkadapu *et al.* [14] of a same chemistry shared by m- and p-xylenes, which is in many aspects very close to that of toluene. In contrast, due to the two ring substituents in ortho-position, the chemistry of o-xylene is very different from that of m- and p-xylenes. Due to the internal isomerization of the peroxy radical obtained by addition to oxygen of resonance stabilized methylbenzyl radical, which is only possible with two methyl groups in ortho-position, o-xylene exhibits a

higher reactivity and the formation of specific types of reaction products, such as phthalan with a NTC behavior, and 2,3-dihydrobenzofuran. Moreover, the production of indene is also favored with o-xylene.

After addition of specific pathways for the formation of 2,3-dihydrobenzofuran, indene, 1,3-benzodioxole, a detailed model combining that for the oxidation of toluene of Yuan et al. [29] and that for the oxidation of xylenes of Kukkadapu et al. [14] with the Galway C_0-C_3 reaction base [32] allows well reproducing the fuel consumption of the four investigated methylated benzenes at the three studied equivalence ratios (0.5, 1 and 2) and reasonably predicting and understanding the formation of most of the 25 quantified products. However, improvements might certainly be obtained using theoretical calculations for the reactions of methylated phenyl and cyclopentadienyl radicals.

An improved detection and quantification of some reaction products might be obtained by using mass spectrometry with molecular beam sampling. This might help to better quantified the products, which were assumed to condensate in the transfer line, e.g. phenol and cresols, or those such formaldehyde, cyclopentadienone, and quinonemethide, which are predicted in significant amounts, but are not experimentally detected using the present analytical procedure; further experiments using mass spectrometry analyses with molecular beam sampling would be of interest to fully prove the validity of the used model.

Acknowledgements

We acknowledge funding from the European Union's Horizon 2020 research and innovation program (BUILDING A LOW-CARBON, CLIMATE RESILIENT FUTURE: SECURE, CLEAN AND EFFICIENT ENERGY) under Grant Agreement No 101006744. The content presented in this document represents the views of the authors, and the European Commission has no liability in respect of the content.

References

[1] J.C. Guibet, Fuels and Engines, TECHNIP, 1997.
[2] M.D. Boot, M. Tian, E.J.M. Hensen, S. Mani Sarathy, Impact of fuel molecular structure on auto-ignition behavior – Design rules for future high performance gasolines, Prog. Energ. Combust. 60 (2017) 1–25.
[3] F. Battin-Leclerc, N. Delort, I. Meziane, O. Herbinet, Y. Sang, Y. Li, Possible use as biofuels of monoaromatic oxygenates produced by lignin catalytic conversion: A review, Catal. Today 408 (2023) 150–167.
[4] H. Jin, W. Yuan, W. Li, J. Yang, Z. Zhou, L. Zhao, Y. Li, F. Qi, Combustion chemistry of aromatic hydrocarbons, Prog. Energ. Combust. 96 (2023) 101076.
[5] V. Vasudevan, D.F. Davidson, R.K. Hanson, Shock tube measurements of toluene ignition times and OH concentration time histories, P. Combust. Inst. 30 (2005) 1155–1163.
[6] D.F. Davidson, B.M. Gauthier, R.K. Hanson, Shock tube ignition measurements of iso-octane/air and toluene/air at high pressures, P. Combust. Inst. 30 (2005) 1175–1182.
[7] H.-P.S. Shen, J. Vanderover, M.A. Oehlschlaeger, A shock tube study of the auto-ignition of toluene/air mixtures at high pressures, P. Combust. Inst. 32 (2009) 165–172.
[8] F. Battin-Leclerc, R. Bounaceur, N. Belmekki, P.A. Glaude, Experimental and modeling study of the oxidation of xylenes, Int. J. Chem. Kinet. 38 (2006) 284–302.
[9] H.-P.S. Shen, M.A. Oehlschlaeger, The autoignition of C8H10 aromatics at moderate temperatures and elevated pressures, Combust. Flame 156 (2009) 1053–1062.
[10] S. Gudiyella, T. Malewicki, A. Comandini, K. Brezinsky, High pressure study of m-xylene oxidation, Combust. Flame 158 (2011) 687–704.
[11] G. Mittal, C.-J. Sung, Autoignition of toluene and benzene at elevated pressures in a rapid compression machine, Combust. Flame 150 (2007) 355–368.
[12] A. Roubaud, R. Minetti, L.R. Sochet, Oxidation and combustion of low alkylbenzenes at high pressure: comparative reactivity and auto-ignition, Combust. Flame 121 (2000) 535–541.
[13] A. Roubaud, O. Lemaire, R. Minetti, L.R. Sochet, High pressure auto-ignition and oxidation mechanisms of o-xylene, o-ethyltoluene, and n-butylbenzene between 600 and 900 K, Combust. Flame 123 (2000) 561–571.
[14] G. Kukkadapu, D. Kang, S.W. Wagnon, K. Zhang, M. Mehl, M. Monge-Palacios, H. Wang, S.S. Goldsborough, C.K. Westbrook, W.J. Pitz, Kinetic modeling study of surrogate

components for gasoline, jet and diesel fuels: C7-C11 methylated aromatics, P. Combust. Inst. 37 (2019) 521–529.
[15] K. Brezinsky, T.A. Litzinger, I. Glassman, The high temperature oxidation of the methyl side chain of toluene, Int. J. Chem. Kinet. 16 (1984) 1053–1074.
[16] K. Brezinsky, A.B. Lovell, I. Glassman, The Oxidation of Toluene Perturbed by NO2, Combust. Sci. Technol. 70 (1990) 33–46.
[17] S.D. Klotz, K. Brezinsky, I. Glassman, Modeling the combustion of toluene-butane blends, Symp. (Int.) Combust. 27 (1998) 337–344.
[18] W.K. Metcalfe, S. Dooley, F.L. Dryer, Comprehensive Detailed Chemical Kinetic Modeling Study of Toluene Oxidation, Energ. Fuel. 25 (2011) 4915–4936.
[19] J.L. Emdee, K. Brezinsky, I. Glassman, Oxidation of O-xylene, Symp. (Int.) Combust. 23 (1991) 77–84.
[20] J.L. Emdee, K. Brezinsky, I. Glassman, High-temperature oxidation mechanisms of m- and p-xylene, J. Phys. Chem. 95 (1991) 1626–1635.
[21] S. Gaïl, P. Dagaut, Experimental kinetic study of the oxidation of p-xylene in a JSR and comprehensive detailed chemical kinetic modeling, Combust. Flame 141 (2005) 281–297.
[22] S. Gaïl, P. Dagaut, Oxidation of m-xylene in a JSR: experimental study and detailed chemical kinetic modeling, Combust. Sci. Technol. 179 (2007) 813–844.
[23] S. Gaïl, P. Dagaut, G. Black, J.M. Simmie, Kinetics of 1,2-Dimethylbenzene Oxidation and Ignition: Experimental and Detailed Chemical Kinetic Modeling, Combust. Sci. Technol. 180 (2008) 1748–1771.
[24] P. Dagaut, G. Pengloan, A. Ristori, Oxidation, ignition and combustion of toluene: Experimental and detailed chemical kinetic modeling, Phys. Chem. Chem. Phys. 4 (2002) 1846–1854.
[25] R. Bounaceur, I. Da Costa, R. Fournet, F. Billaud, F. Battin-Leclerc, Experimental and modeling study of the oxidation of toluene, Int. J. Chem. Kinet. 37 (2005) 25–49.
[26] W. Yuan, Y. Li, P. Dagaut, J. Yang, F. Qi, Investigation on the pyrolysis and oxidation of toluene over a wide range conditions. I. Flow reactor pyrolysis and jet stirred reactor oxidation, Combust. Flame 162 (2015) 3–21.
[27] W. Yuan, L. Zhao, S. Gaïl, J. Yang, Y. Li, F. Qi, P. Dagaut, Exploring pyrolysis and oxidation chemistry of o-xylene at various pressures with special concerns on PAH formation, Combust. Flame 228 (2021) 351–363.
[28] W. Yuan, L. Zhao, J. Yang, Z. Zhou, Y. Li, F. Qi, Insights into the Decomposition and Oxidation Chemistry of p-Xylene in Laminar Premixed Flames, J. Phys. Chem. A. 125 (2021) 3189–3197.
[29] W. Yuan, Y. Li, P. Dagaut, J. Yang, F. Qi, Investigation on the pyrolysis and oxidation of toluene over a wide range conditions. II. A comprehensive kinetic modeling study, Combust. Flame 162 (2015) 22–40.
[30] S. Namysl, M. Pelucchi, L. Pratali Maffei, O. Herbinet, A. Stagni, T. Faravelli, F. Battin-Leclerc, Experimental and modeling study of benzaldehyde oxidation, Combust. Flame 211 (2020) 124–132.
[31] I. Meziane, Y. Fenard, N. Delort, O. Herbinet, J. Bourgalais, A. Ramalingam, K.A. Heufer, F. Battin-Leclerc, Experimental and modeling study of acetone combustion, Combust. Flame (2022) 112416.
[32] U. Burke, W.K. Metcalfe, S.M. Burke, K.A. Heufer, P. Dagaut, H.J. Curran, A detailed chemical kinetic modeling, ignition delay time and jet-stirred reactor study of methanol oxidation, Combust. Flame 165 (2016) 125–136.

[33] R.D. Büttgen, M. Tian, Y. Fenard, H. Minwegen, M.D. Boot, K.A. Heufer, An experimental, theoretical and kinetic modelling study on the reactivity of a lignin model compound anisole under engine-relevant conditions, Fuel 269 (2020) 117190.
[34] S.W. Wagnon, S. Thion, E.J.K. Nilsson, M. Mehl, Z. Serinyel, K. Zhang, P. Dagaut, A.A. Konnov, G. Dayma, W.J. Pitz, Experimental and modeling studies of a biofuel surrogate compound: laminar burning velocities and jet-stirred reactor measurements of anisole, Combust. Flame 189 (2018) 325–336.
[35] M. Nowakowska, O. Herbinet, A. Dufour, P.A. Glaude, Kinetic Study of the Pyrolysis and Oxidation of Guaiacol, J. Phys. Chem. A. 122 (2018) 7894–7909.
[36] A. Burcat, C. Snyder, T. Brabbs, Ignition Delay Times of Benzene and Toluene with Oxygen in Argon Mixtures, National Aeronautics and Space Administration, National Aeronautics and Space Administration Lewis Research Center, Cleveland, Ohio 44135, 1985.
[37] G. Pengloan, Etude cinétique de l'oxydation de composés aromatiques: application à la formation de polluants dans les moteurs automobiles, PhD Thesis, Orléans, 2001.
[38] D. Han, S. Deng, W. Liang, P. Zhao, F. Wu, Z. Huang, C.K. Law, Laminar flame propagation and nonpremixed stagnation ignition of toluene and xylenes, P. Combust. Inst. 36 (2017) 479–489.
[39] G. Wang, Y. Li, W. Yuan, Z. Zhou, Y. Wang, Z. Wang, Investigation on laminar burning velocities of benzene, toluene and ethylbenzene up to 20 atm, Combust. Flame 184 (2017) 312–323.
[40] Y. Zhang, Q. Li, H. Liu, Z. Yan, Z. Huang, Comparative study on the laminar flame speeds of methylcyclohexane-methanol and toluene-methanol blends at elevated temperatures - ScienceDirect, Fuel 245 (2019) 534–543.
[41] B.-J. Zhong, H.-S. Peng, D. Zheng, The effect of different class of hydrocarbons on laminar flame speeds of three C7 fuels, Fuel 225 (2018) 225–229.
[42] R.J. Johnston, J.T. Farrell, Laminar burning velocities and Markstein lengths of aromatics at elevated temperature and pressure, P. Combust. Inst. 30 (2005) 217–224.
[43] S.G. Davis, H. Wang, K. Breinsky, C.K. Law, Laminar flame speeds and oxidation kinetics of benene-air and toluene-air flames, Symp. (Int.) Combust. 26 (1996) 1025–1033.
[44] S.G. Davis, C.K. Law, Determination of and Fuel Structure Effects on Laminar Flame Speeds of C1 to C8 Hydrocarbons, Combust. Sci. Technol. 140 (1998) 427–449.
[45] T. Hirasawa, C.J. Sung, A. Joshi, Z. Yang, H. Wang, C.K. Law, Determination of laminar flame speeds using digital particle image velocimetry: Binary Fuel blends of ethylene, n-Butane, and toluene, P. Combust. Inst. 29 (2002) 1427–1434.
[46] C. Ji, E. Dames, H. Wang, F.N. Egolfopoulos, Propagation and extinction of benzene and alkylated benzene flames, Combust. Flame 159 (2012) 1070–1081.
[47] K. Kumar, C.-J. Sung, Flame Propagation and Extinction Characteristics of Neat Surrogate Fuel Components, Energ. Fuel. 24 (2010) 3840–3849.
[48] X. Hui, A.K. Das, K. Kumar, C.-J. Sung, S. Dooley, F.L. Dryer, Laminar flame speeds and extinction stretch rates of selected aromatic hydrocarbons, Fuel 97 (2012) 695–702.
[49] X. Hui, C.-J. Sung, Laminar flame speeds of transportation-relevant hydrocarbons and jet fuels at elevated temperatures and pressures, Fuel 109 (2013) 191–200.
[50] C. Ji, F.N. Egolfopoulos, Flame propagation of mixtures of air with binary liquid fuel mixtures, P. Combust. Inst. 33 (2011) 955–961.

[51] Y.-H. Liao, W.L. Roberts, Laminar Flame Speeds of Gasoline Surrogates Measured with the Flat Flame Method, Energ. Fuel. 30 (2016) 1317–1324.
[52] L. Sileghem, V.A. Alekseev, J. Vancoillie, K.M. Van Geem, E.J.K. Nilsson, S. Verhelst, A.A. Konnov, Laminar burning velocity of gasoline and the gasoline surrogate components iso-octane, n-heptane and toluene, Fuel 112 (2013) 355–365.
[53] P. Dirrenberger, P.A. Glaude, R. Bounaceur, H. Le Gall, A.P. da Cruz, A.A. Konnov, F. Battin-Leclerc, Laminar burning velocity of gasolines with addition of ethanol, Fuel 115 (2014) 162–169.
[54] L. Dupont, H.Q. Do, G. Capriolo, A.A. Konnov, A. El Bakali, Experimental and kinetic modeling study of para-xylene chemistry in laminar premixed flames, Fuel 239 (2019) 814–829.
[55] J.D. Munzar, B. Akih-Kumgeh, B.M. Denman, A. Zia, J.M. Bergthorson, An experimental and reduced modeling study of the laminar flame speed of jet fuel surrogate components, Fuel 113 (2013) 586–597.
[56] Y. Wu, B. Rossow, V. Modica, X. Yu, L. Wu, F. Grisch, Laminar flame speed of lignocellulosic biomass-derived oxygenates and blends of gasoline/oxygenates, Fuel 202 (2017) 572–582.
[57] M.B. Colket, D.J. Seery, Reaction mechanisms for toluene pyrolysis, Symp. (Int.) Combust. 25 (1994) 883–891.
[58] R. Sivaramakrishnan, R.S. Tranter, K. Brezinsky, High-pressure, high-temperature oxidation of toluene, Combust. Flame 139 (2004) 340–350.
[59] R. Sivaramakrishnan, R.S. Tranter, K. Brezinsky, High Pressure Pyrolysis of Toluene. 1. Experiments and Modeling of Toluene Decomposition, J. Phys. Chem. A. 110 (2006) 9388–9399.
[60] W. Sun, A. Hamadi, F.E.C. Ardila, S. Abid, N. Chaumeix, A. Comandini, Insights into pyrolysis kinetics of xylene isomers behind reflected shock waves, Combust. Flame 244 (2022) 112247.
[61] Y. Li, J. Cai, L. Zhang, T. Yuan, K. Zhang, F. Qi, Investigation on chemical structures of premixed toluene flames at low pressure, P. Combust. Inst. 33 (2011) 593–600.
[62] L. Zhao, Z. Cheng, L. Ye, F. Zhang, L. Zhang, F. Qi, Y. Li, Experimental and kinetic modeling study of premixed o-xylene flames, P. Combust. Inst. 35 (2015) 1745–1752.
[63] CHEMKIN 10112, Reaction Design, (2011).
[64] A. Stagni, Y. Song, L.A. Vandewalle, K.M. Van Geem, G.B. Marin, O. Herbinet, F. Battin-Leclerc, T. Faravelli, The role of chemistry in the oscillating combustion of hydrocarbons: An experimental and theoretical study, Chem. Eng. J. 385 (2020) 123401.
[65] T. Seta, M. Nakajima, A. Miyoshi, High-Temperature Reactions of OH Radicals with Benzene and Toluene, J. Phys. Chem. A. 110 (2006) 5081–5090.
[66] G. da Silva, C.-C. Chen, J.W. Bozzelli, Toluene Combustion: Reaction Paths, Thermochemical Properties, and Kinetic Analysis for the Methylphenyl Radical + O2 Reaction, J. Phys. Chem. A. 111 (2007) 8663–8676.
[67] M.U. Alzueta, M. Oliva, P. Glarborg, Parabenzoquinone pyrolysis and oxidation in a flow reactor, Int. J. Chem. Kinet. 30 (1998) 683–697.
[68] L.-S. Tran, O. Herbinet, H.-H. Carstensen, F. Battin-Leclerc, Chemical kinetics of cyclic ethers in combustion, Prog. Energ. Combust. 92 (2022) 101019.